



Microwave-assisted depolymerisation of organosolv lignin via mild hydrogen-free hydrogenolysis: Catalyst screening

Ana Toledano ^a, Luis Serrano ^a, Antonio Pineda ^b, Antonio A. Romero ^b, Rafael Luque ^{b,*}, Jalel Labidi ^{a,**}

^a Environmental and Chemical Engineering Department, University of the Basque Country, Plaza Europa, 1, 20018 Donostia-San Sebastián, Spain

^b Departamento de Química Orgánica, Universidad de Córdoba, Ctra Nnal IV-A, Km 396, E-14014 Córdoba, Spain

ARTICLE INFO

Article history:

Received 7 August 2012

Received in revised form 9 October 2012

Accepted 14 October 2012

Available online 23 October 2012

Keywords:

Organosolv lignin

Hydrogenolysis

Lignin depolymerisation

Heterogeneous catalysis

ABSTRACT

Lignin depolymerisation to simple aromatics was investigated by using a mild microwave-assisted approach. The reaction was catalysed by different supported metal nanoparticles on mesoporous Al-SBA-15 including -nickel (2, 5 and 10 wt.%), palladium (2 wt.%), platinum (2 wt.%) and ruthenium (2 wt.%). Three main products were identified in the proposed lignin valorisation protocol, namely a bio-oil, a bio-char and a fraction of residual lignin. These have been characterised by means of several techniques including GC-MS, MALDI-TOF, HPSEC and elemental analysis in order to evaluate the extension and mechanism of the selected depolymerisation approach. In this work, the objective has been the maximisation of bio-oil yield as well as its content in phenolic monomeric compounds. All tested catalysts exhibited improved results as compared to the blank depolymerisation (without catalyst), demonstrating a synergistic effect of metal nanoparticles in lignin hydrogenolysis. The most abundant phenolic products observed in most studied catalysts have been solvent derived products such as diethyl phthalate and butyl-octyl phthalate ester. Interestingly, phenolic compounds derived from lignin were also obtained including mesitol and syringaldehyde as well as desapidinol and aspidinol, depending on the utilised solvent in the systems. The bio-oil obtained was primarily composed of monomers, dimers and trimers. Biochar yield was relatively high in most cases (>35% in some cases) due to existing oligomerisation reactions under the investigated conditions except for the case of the use of formic acid which gave no biochar in the process. Residual lignin content was often high and repolymerisation was observed in some cases. The catalyst containing 10 wt.% nickel was confirmed to achieve the highest lignin depolymerisation degree, with a maximum yield of 30% bio-oil after a short time of reaction (typically 30 min of microwave irradiation).

© 2012 Elsevier B.V. All rights reserved.

1. Introduction

Lignin is a natural phenolic macromolecule present in vegetal cell walls comprising of three main phenylpropane units, namely guaiacyl alcohol (G), syringyl alcohol (S) and *p*-coumaryl alcohol (H) [1]. Lignin has a highly complex structure which consists of a 3D randomised net linked to hemicelluloses (LCC), functioning as a biological barrier and as glue to retain linked hemicelluloses and celluloses. Tonnes of lignins are readily available from the pulp and paper industries and such quantities are expected to increase by the implementation of second generation bioethanol plants. Profiting from its unique structure in nature, lignin holds a significant potential to be valorised to produce phenolic platform chemicals. In view of these premises, lignin valorisation practises to produce

high added value phenolic compounds have recently attracted a great deal of attention from the scientific community.

A wide range of chemical transformations can be envisaged to produce aromatic compounds from lignin. These have been generally based on two main approaches: *oxidation* and *hydrotreating* (hydrogenolysis) related protocols [2,3]. In some cases, degradation with enzyme cocktails have also been described [4]. However, depolymerisation processes are often not well understood. Taking a look at general methodologies and recently reported protocols, there are two main considerations that should be taken into account for lignin valorisation purposes, which most of the literature reports have generally overlooked to date. These include (1) a maximisation of the activity of the catalyst under the chosen conditions (as mild as possible), bearing in mind the bulky nature of this recalcitrant biomass source and (2) most importantly repolymerisation and self-condensation capability of lignin under processing conditions (due to the formation of radicals [5] and/or C–C bond forming self-condensation reactions in acidic media [6]) which may eventually lead to a complex pool of poorly

* Corresponding author. Tel.: +34 957211050; fax: +34 957212066.

** Corresponding author. Tel.: +34 943017178; fax: +34 94301714.

E-mail addresses: q62alsor@uco.es (R. Luque), jalel.labidi@ehu.es (J. Labidi).

controllable re-condensed aromatics as demonstrated by several groups worldwide [2,5–7]. In other cases, depolymerisation is more or less achieved giving a series of relatively simple aromatics under generally harsh reaction conditions (high hydrogen pressures, temperatures >400 °C) with low yields to products (<50%) [2,3,6,8,9]. Another important aspect to consider is the addition of hydrogen in the systems, which is generally not avoided or controlled in most cases and could lead to an undesirable partial or complete hydrogenation of the aromatic rings in the presence of metal sites [10]. This will contribute not only to a poor hydrogen economy of the methodology but also to less interesting and low value compounds [11].

The use of oxidants and/or oxidising protocols is in principle totally undesirable as the presence of radicals will lead to partial re-polymerisation of lignin and thus to more complex structures. In contrast, reactions under hydrotreating conditions may favour quenching and recombination of radicals, minimising lignin repolymerisation side reactions while maximising C–O bond cleavage. Previous work and results in this field point to a general consensus in catalytic hydrogenolysis methodologies as a valuable approach to unravel structural features of lignin through the production of lignin degradation products [12].

In any case, the design of a system able to work under mild reaction conditions without the addition of molecular hydrogen (e.g. the use of hydrogen donating solvents) will offer a significant advantage to improve the green credentials of the process. The hydrogen-donating effect of certain solvents (e.g. tetralin) in the hydrocracking of kraft lignin was established by Connor et al. in the early 80s [13]. The advantages of tetralin as hydrogen-donor solvent included a high boiling point as well as the swift and efficient generation of hydrogen under hydrocracking conditions which leads to the formation of naphthalene, a relatively stable compound. In Thring's proposed approach, phenols, guaiacols, syringols, catechols and aldehydes were obtained as major products from lignin [14].

In this work, we disclose a novel microwave-assisted mild hydrogenolytic methodology to depolymerise organosolv lignin from olive tree pruning into simple phenolic compounds. With this purpose, a range of catalysts based on metal supported

nano particles on mesoporous acidic aluminosilicate supports (Al-SBA-15) with typical metal loadings of 2 wt.% have been prepared using a novel mechanochemical approach developed in our group [15]. Nickel catalysts were also tested at higher concentrations (5 and 10 wt.%).

The bifunctional catalysts were rationally designed from a fundamental understanding point of view to maximise lignin depolymerisation under the investigated conditions. These include (1) the maximisation of the accessibility and activity of the metal sites (supported metal nanoparticles synthesised by ball milling have been proved to predominantly deposit in the external surface of a support being highly active and accessible even at very low loadings [15]) as well as (2) the minimisation of repolymerisation and related side reactions (by using a mild hydrogenolytic approach under reducing conditions that can in principle quench radicals and unstable intermediates formed during depolymerisation) which avoids, at the same time, the addition of hydrogen in the systems. Al-SBA-15 was chosen as support due to its good (hydro)thermal stability, large surface area (useful for the deposition of nanoparticles) and most importantly combination of moderate Brønsted and Lewis acidity which is a pre-requisite to promote dealkylations, deacetylations and related chemistries involved in the production of simple aromatics generated in lignin valorisation practises [6].

2. Materials and methods

2.1. Lignin isolation

Olive tree pruning (*Olea europaea*, variety Arróniz) was utilised as feedstock to isolate lignin. The treatment for lignin extraction consisted on the digestion of the feedstock in a mixture of ethanol–water (70 wt.%) at 200 °C for 90 min (previous optimised conditions [16]) in a pressure reactor. The liquid fraction (where lignin was dissolved) was separated from the solid fraction by filtration. Dissolved lignin was isolated by precipitation with two acidified portions of an aqueous solution (pH around 2). The suspension was centrifuged at 4000 rpm for 20 min to recover lignin which was then dried at 50 °C. Organosolv olive tree pruning lignin possessed the following composition: acid insoluble

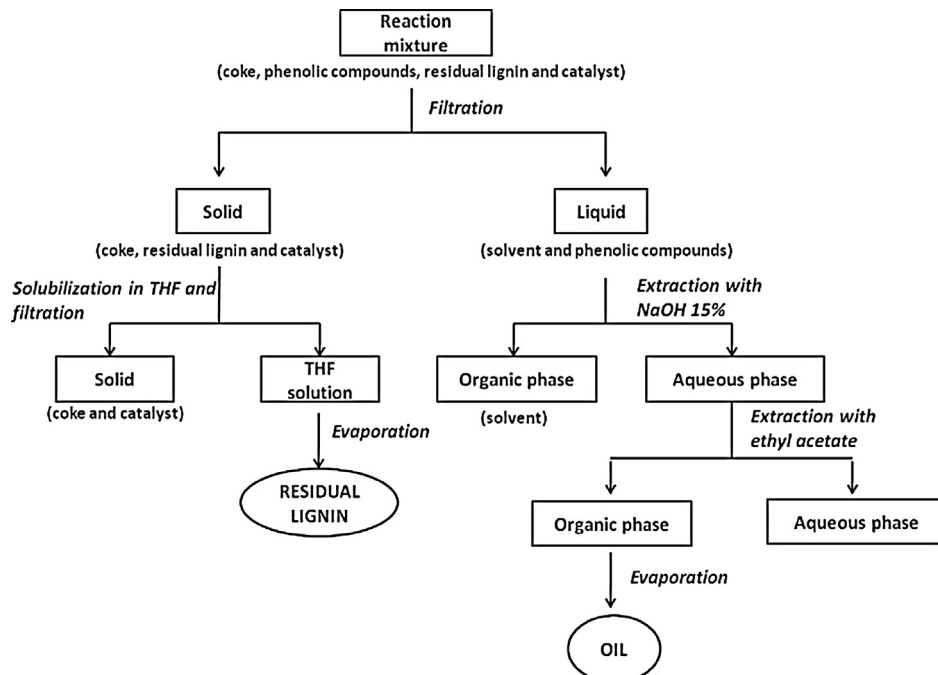


Fig. 1. Reaction mixture separation procedure.

lignin $71.90\% \pm 0.79$, acid soluble lignin $1.63\% \pm 0.08$, total sugars $2.94\% \pm 0.14$ (glucose $1.75\% \pm 0.12$, xylose $1.10\% \pm 0.03$ and arabinose $0.09\% \pm 0.01$) and ash content $0.39\% \pm 0.01$.

2.2. Lignin depolymerisation reactions

Hydrogenolysis reactions were carried out in a multimode microwave reaction system Milestone ETHOS-1. Tetralin (or alternatively formic acid) were used as hydrogen donor solvent due to their possibility to generate hydrogen in situ upon heating as well as producing naphthalene as stable product that does not interfere in lignin hydrogenolysis [13]. In a typical reaction, the microwave vessel was filled with a lignin:catalyst ratio of 1:1 and a solid:liquid ratio of 1:12.5. A blank experiment (without catalyst) was carried out as control. Microwave power was set constant at 400 W over 30 min, and reactions reached an average temperature of 140 °C for all experiments.

A scheme of the product separation is provided in Fig. 1. The yield of every product was calculated gravimetrically as referred to the initial lignin content.

2.3. Catalyst synthesis and characterisation

The studied catalysts were prepared following a previously reported novel dry mechanochemical approach [16]. In a typical synthesis, 0.2 g Al-SBA-15 was grinded with the needed quantity (to reach a theoretical 2 wt.% metal) of metal precursor (NiCl_2 , $\text{Pd}(\text{AcO})_2$, $\text{Pt}(\text{NH}_3)(\text{NO}_3)_2$ and $\text{RuCl}_3 \cdot \text{H}_2\text{O}$) in a Retsch PM-100 planetary ball mill using a 125 mL reaction chamber and 10 mm stainless steel balls. Milling conditions were 10 min at 350 rpm (optimised conditions). Upon milling, as-synthesised materials were conditioned to remove the excess of unreacted and/or physisorbed precursor and directly calcined at 400 °C under air for 4 h. Prior to the reaction, the catalysts were activated and reduced in a flow of hydrogen/helium (50 mL min^{-1}) for 1 h. Materials were filtered off after reaction, thoroughly washed with THF (to remove residual lignin from pores and/or surface) and oven dried overnight at 150 °C to ensure the removal of all physisorbed compounds from the catalyst, prior to their reuse in the reaction.

The prepared catalyst, denoted as Ni2%AlSBA, Ni5%AlSBA, Ni10%AlSBA, Pd2%AlSBA, Pt2%AlSBA and Ru2%AlSBA, were subsequently characterised by a number of techniques including X-ray Diffraction (XRD), N₂ physisorption, TEM, EDX, Inductively Coupled Plasma (ICP, for metal determination) and X-ray Photoelectron Spectroscopy (XPS).

XRD patterns were collected on a Siemens D-5000 diffractometer (40 kV, 30 mA) equipped with a Ni filter and a graphite monochromator, using Cu K_α radiation ($\lambda = 1.54 \text{ \AA}$). Scans were performed in the 10–80° range at a step time of 0.040 at 1° min^{-1} .

Nitrogen adsorption measurements were carried out at 77 K using an ASAP 2010 volumetric adsorption analyser from Micromeritics. The samples were outgassed for 2 h at 100 °C under vacuum ($p < 10^{-2} \text{ Pa}$) and subsequently analysed. The linear part of the BET equation (relative pressure between 0.05 and 0.22) was used for the determination of the specific surface area.

TEM micrographs were recorded on a FEI Tecnai G2 fitted with a CCD camera for ease and speed of use. The resolution is around 0.4 nm. Samples were suspended in ethanol and deposited straight away on a copper grid prior to analysis.

XPS (aka ESCA) measurements were performed in a ultra high vacuum (UHV) multipurpose surface analysis system (Specs™ model, Germany) operating at pressures $< 10^{-10} \text{ mbar}$ using a conventional X-ray source (XR-50, Specs, Mg-K_α, 1253.6 eV) in a "stop-and-go" mode to reduce potential damage due to sample irradiation. The survey and detailed Fe and Cu high-resolution spectra (pass energy 25 and 10 eV, step size 1 and 0.1 eV, respectively)

were recorded at room temperature with a Phoibos 150-MCD energy analyser. Powdered samples were deposited on a sample holder using double-sided adhesive tape and subsequently evacuated under vacuum ($< 10^{-6} \text{ Torr}$) overnight. Eventually, the sample holder containing the degassed sample was transferred to the analysis chamber for XPS studies. Binding energies were referenced to C1s (284.6 eV) from adventitious carbon. The curve deconvolution of the obtained XPS spectra was obtained using the Casa XPS program.

The metal content in the materials was determined using Inductively Coupled Plasma (ICP) in a Philips PU 70000 sequential spectrometer equipped with an Echelle monochromator (0.0075 nm resolution). Samples were digested in HNO₃ and subsequently analysed by ICP at the SCAI (Universidad de Córdoba).

Further details on catalyst characterisation are included in subsequent sections as well as in the ESI.

2.4. Products characterisation

The obtained bio-oil was characterised in order to establish the nature and structures of the contained monomeric phenolic compounds and to determine the molecular weight profile. The bio-oil was dissolved in ethyl acetate (HPLC grade) in a metric flask and then injected in a GC (7890A)-MS (5975D inert MSD with Triple-Axis Detector) Agilent equipped with a capillary column HP-5MS [(5%-phenyl)-methylpolysiloxane, 60 m × 0.32 mm]. The temperature programme started at 50 °C, then the temperature was increased to 120 °C at 10° C/min (held 5 min at this temperature), increased to 280 °C at 10° C/min (8 min hold at this temperature), increased to 300 °C at 10° C/min (held 2 min at this temperature). Helium was employed as carrier gas. Samples were quantified using phenol as internal standard.

Matrix assisted Laser desorption/ionisation time-of-flight mass spectrometry (MALDI-TOF) was conducted to check the molecular weight distribution of the bio-oil in a Voyager-DE™ STR Biospectrometry™ Workstation of Applied Biosystems. The technique was also useful to ascertain the degree of depolymerisation in the experiments. A 15 g/L solution of DABP (3,4-diaminobenzophenone) in a methanol–water mixture (8:2) was used as matrix. The analyses were developed in negative mode.

Residual lignin was subjected to High Performance Size Exclusion Chromatography (HPSEC) to evaluate lignin molecular weight (MW) and molecular weight distribution (MWD) using a JASCO instrument equipped with an interface (LC-NetII/ADC) and a refractive index detector (RI-2031Plus). Two PolarGel-M columns (300 × 7.5 mm) and PolarGel-M guard (50 × 7.5 mm) were employed. Dimethylformamide + 0.1% lithium bromide was used as eluent. The flow rate was 0.7 mL min^{-1} and the analyses were carried out at 40 °C. Calibration was made using polystyrene standards (Sigma–Aldrich) ranging from 266 to 70,000 g mol⁻¹.

An elemental analyser EuroEA 3000 (Eurovector, Italia) was utilised to carry out CHN and CHNS analyses. Parameters: carrier flow: 115 mL min^{-1} , oxygen 15 mL, source temperature 980 °C, column oven temperature (GC Column SS 2 m 6 × 5 mm) 100 °C.

3. Results and discussion

3.1. Catalysts properties and characteristics

A series of considerations for the rational design of heterogeneous catalysts for lignin depolymerisation practises using heterogeneous catalysts should be taken into account prior to any experiments. Contrary to most reports to date in which Rh, Pt and Pd-based catalysts were the most widely employed in the transformations of lignin model compounds [6,9,17], the

Table 1

Textural properties, metal content and nanoparticle sizes of the various investigated supported metal nanoparticles in the depolymerisation of crude lignin.

| Catalyst | Textural properties | | | Metal content | | | NP size (nm) ^a | |
|--------------|---|-----------------------------------|--------------------|----------------|------------|------------|---------------------------|------------------|
| | S_{BET} ($\text{m}^2 \text{g}^{-1}$) | Pore volume (mLg^{-1}) | Pore diameter (nm) | ICP (wt.%) | EDX (wt.%) | XPS (wt.%) | TEM ^b | XRD ^c |
| Al-SBA-15 | 804 | 1.03 | 8.2 | — | — | — | — | — |
| Ni2%AlSBA | 614 | 1.01 | 7.5 | 1.84 | 1.63 | 1.79 | 32 | 42 |
| Ni5%AlSBA | 642 | 0.96 | 7.7 | 4.72 | 3.01 | 3.45 | 20 | 25 |
| Ni10%AlSBA | 642 | 1.00 | 7.4 | 9.32 | 4.57 | 5.05 | 29 | 40 |
| Ni10%-reused | 506 | 0.86 | 7.2 | 9.05 | 4.78 | 4.52 | 34 | 45 |
| Pd2%AlSBA | 617 | 0.91 | 7.6 | 1.75 | 2.97 | 1.64 | 5 | 8 |
| Pt2%AlSBA | 600 | 0.98 | 7.3 | 1.76 | 1.20 | 1.35 | — ^d | 37 |
| Ru2%AlSBA | 520 | 0.71 | 6.7 | — ^b | 1.26 | 1.67 | — ^d | 17 |

^a Average nanoparticle size from TEM (averaging >50 NPs).

^b Averaged NPs size counting 50 nanoparticles from TEM images (excluding large aggregates).

^c Calculated using the Scherrer equation.

^d Not measured.

promising potential of Ni catalysts in C–O bond cleavage combined with a suitably designed acidic support for subsequent C–C bond cleavage of the compounds obtained from lignin has been highlighted in this work [9,18,19].

Li et al. recently reported the use of a carbon supported Ni-W₂C catalyst for the direct catalytic conversion of raw woody biomass (e.g. birch, poplar, pine and related feedstocks) into monophenols up to 46.5% yield (based on lignin) without any pretreatment step [9]. These authors showed this type of catalyst exhibited a comparable activity to that of noble metals, paving the way to a further development of Ni-based materials for lignin depolymerisation.

Table 1 summarises the properties of the investigated catalysts. All materials maintained high surface areas, pore volumes and pore diameters from the parent aluminosilicate, with reduced values due to the partial deposition of metal nanoparticles on the support. The deposition of nanoparticles was predominantly found to take place on the external surface of the support and not within the porous network as indicated by ICP and XPS results, in good agreement with the little reduction of pore diameters and pore volumes observed even at large metal loadings (e.g. Ni10%AlSBA). These results were in good agreement with previous reports from the group [15,20]. In any case, at larger metal loadings (5 wt.% and above) a significant proportion of metal sites are believed to be embedded within the porous network as suggested by the remarkable differences in metal content detected by EDX and XPS (surface techniques) as compared by ICP (digestion of the actual catalyst). NPs sizes were worked out from TEM micrographs as well as for XRD patterns (using the Scherrer equation) and showed, in general, a relative agreement between TEM and XRD data (**Table 1**). Revisiting the actual structure of the catalysts with additional experiments using High Annular Dark Field Scanning Electron Microscopy (HAADF-STEM, see supporting information), some large aggregates could be observed in most materials, particularly those obtained for larger loadings (Ni10%AlSBA), indicating that these may be correlated to the existing differences of averaged NP sizes in TEM (for which aggregates were not accounted) and XRD patterns (which show average NP sizes of in principle all particles).

All catalysts were found to contain metals in their reduced metal state as clearly shown in XRD patterns (**Fig. 2**) and XPS data (**Table 2**) [21]. The supported metal nanoparticles were homogeneously dispersed and clearly visible as depicted in TEM micrographs from **Fig. 3**, although these were not very visible at low metal loadings (2 wt.%, **Fig. 3A**). This even distribution was also maintained at higher metal loadings (**Fig. 3B** for Ni10%AlSBA), although for these materials some larger aggregates (>100 nm) could be observed in some areas (**Fig. 3C** and Supporting information). In the case of Ni10%AlSBA, interesting cubical nanoparticle shapes were also found, which are yet to be investigated if these shapes and/or large

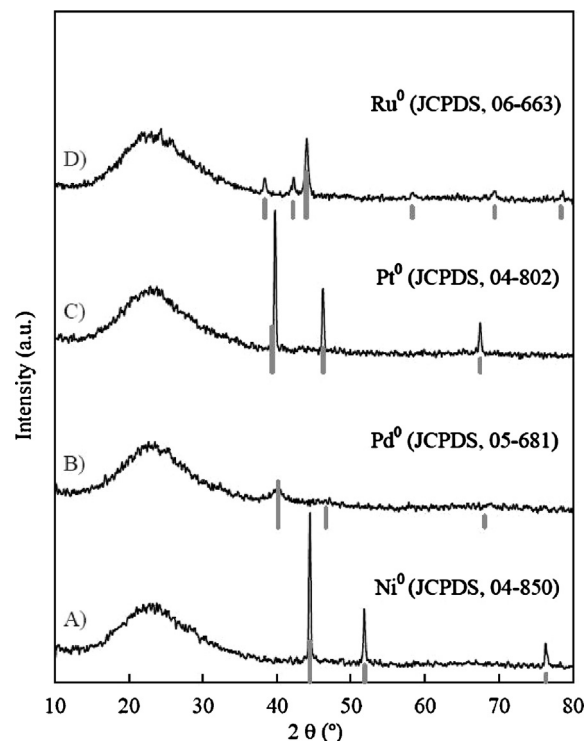


Fig. 2. XRD patterns of 2 wt.% materials; from bottom to top (A) Ni2%AlSBA; (B) Pd2%AlSBA; (C) Pt2%AlSBA; and (D) Ru2%AlSBA. Grey solid lines indicate the different diffraction lines corresponding to the respective metal phases.

particle sizes can influence the activity of the materials in lignin depolymerisation. The mesoporous hexagonal channels of the parent Al-SBA-15 support were preserved in all cases regardless of the quantity and type of metal in the systems, even for the reused catalysts.

Table 2

XPS data of the prepared catalysts including the main lines for the different metal nanoparticles.

| Catalyst | XPS main lines (eV) Metal |
|------------|--|
| Ni2%AlSBA | Ni2p _{3/2} (853.6 eV)–Ni ⁰ |
| Ni5%AlSBA | Ni2p _{3/2} (854.2 eV)–Ni ⁰ |
| Ni10%AlSBA | Ni2p _{3/2} (854.0 eV)–Ni ⁰ |
| Pd2%AlSBA | Pd3d _{3/2} (338.9 eV)–Pd ⁰ |
| Pt2%AlSBA | Pt4f _{5/2} (74.8 eV)–Pt ⁰ |
| Ru2%AlSBA | Ru3d _{3/2} (278.7 eV)–Ru ⁰ |

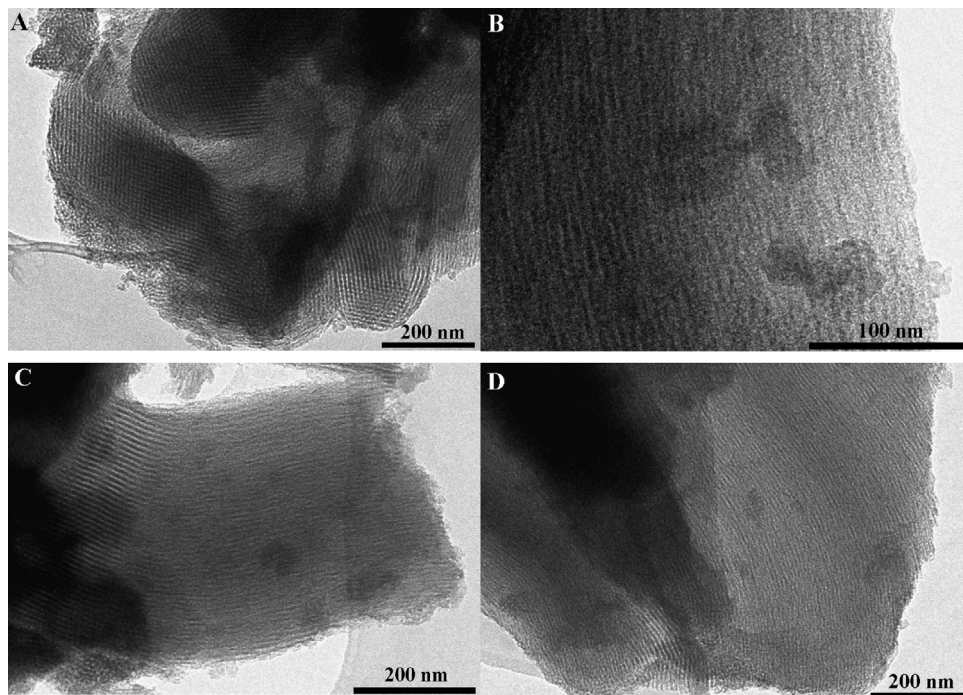


Fig. 3. TEM micrographs of (A) Ni2%AlSBA; (B) Ni10%AlSBA (Ni nanoparticles can be spotted as little black dots); (C) Ni10%AlSBA showing some NP aggregates; and (D) reused Ni10%AlSBA, showing a clearly preserved ordered mesoporous hexagonal channel network after reaction.

These reused materials after reaction exhibited relatively similar textural properties to those of the fresh catalyst (Ni10%AlSBA), although a certain decrease in surface area and pore volume was noticeable in the reused catalyst as well as some decrease in acidity in the systems (about 20%, results not shown). However, results clearly indicate there is certainly no pore collapse in the catalysts after reaction. TEM micrographs of the catalysts before and after reaction (Fig. 3D, see also ESI) also confirmed the preservation of the long range mesoporous order of Al-SBA-15 in the reused catalyst and the presence of similarly large cluster aggregates (>100 nm) together with smaller nanoparticles (see ESI, Fig. S2).

A catalyst screening of the supported metal nanoparticles was then carried out in the depolymerisation of organosolv lignin isolated from olive tree pruning. Three main fractions, apart from gaseous products (that were not quantified in the systems), were obtained: a bio-oil enriched in phenolics, a bio-char and a residual lignin. The obtained products (bio-oil) and by-products (bio-char and residual lignin) were analysed in order to determine their composition as well as to find out the effect of the nature of the reduced metal employed on yields to phenolic monomers and bio-char.

3.2. Bio-oil yield and composition

Phenolic compounds were recovered and isolated as a bio-oil in order to study the influence of the catalyst on its yield and composition. Table 3 shows bio-oil yields in the different catalytic systems as referred to initial lignin weight (wt.%). All catalysts were found to provide improved results as compared to blank runs (without catalyst), indicating the positive effect of the catalyst on lignin hydrogenolysis. However, interesting differences were observed depending on the supported metal. Nickel catalysts provided improved bio-oil yields as compared to the other metals, in good agreement with recent reports [11,18]. The highest bio-oil yield (17%) using tetralin as hydrogen-donating solvent was obtained when Ni10%AlSBA was utilised as catalyst in lignin hydrogenolysis, its activity being remarkably superior to that of the other studied catalysts. Unexpectedly, palladium-based

catalyst exhibited the lowest oil yield (5 wt.%) in spite of the remarkably smaller nanoparticle sizes (5–6 nm) obtained for this material (see Supporting information) and its excellent hydrogenation properties. However, given the large differences observed in NP sizes as compared to other catalysts investigated in the reaction (5–6 vs 35–40 nm), we believe the presence of these larger NP sizes may be convenient for an improved interaction of the metal sites with lignin due to the bulky structure of lignin (with the possibility of the metal nanoparticles to target various hydrogenolytic neighbouring sites of the complex lignin molecule). This multiple interaction will not be possible in catalysts containing small NPs sizes, thus leading to lower bio-oil production. Furthermore, the presence of some of such small Pd NPs within the pores of the aluminosilicate support (as opposed to those larger nanocrystallites which are undoubtedly deposited on the external surface of the catalyst) which could in principle make them less accessible to lignin (and thus giving low or no activity) cannot be ruled out. Further investigations are currently ongoing in this regard to find additional evidences for the aforementioned hypotheses.

In any case, another hydrogen-donating solvent (formic acid, FA) was investigated in the hydrogenolysis of organosolv lignin which showed an almost double bio-oil yield (~30%) under identical conditions with the additional advantage of a negligible bio-char generation in the systems upon FA decomposition into CO, $\text{CO}_2 + \text{H}_2$ (Table 3). In good agreement with these results, GC traces of the microwave hydrogenolitic experiments using tetralin and formic acid depicted in Fig. 4 highlight the clean, efficiency and simplicity of our proposed methodology in producing a range of simple aromatics which predates any previous lignin depolymerisation heterogeneously catalysed hydrogenolytic reports [22–24].

The difference to 100 observed in Table 3 corresponded to gaseous products [11]. Gaseous yields produced in the thermolysis of kraft lignin using tetralin as hydrogen donating solvent under hydrocracking conditions have been reported to strongly depend on the severity of the treatment [13]. The gaseous products generated in this work were not recovered for further identification

Table 3Products yields (% w/w) referred to initial lignin weight.^a

| | Blank run | Ni2%AlSBA | Ni5%AlSBA | Ni10%AlSBA | Pd2%AlSBA | Pt2%AlSBA | Ru2%AlSBA |
|-----------------|-----------|-----------|-----------|------------|-----------|-----------|-----------|
| Bio-oil | 3.32 | 9.10 | 7.26 | 16.94 | 5.00 | 6.81 | 7.19 |
| Bio-char | 20.10 | 20.26 | 14.70 | 38.11 | 16.89 | 21.85 | 4.31 |
| Residual lignin | 76.49 | 69.82 | 65.94 | 29.65 | 59.76 | 62.92 | 73.57 |

^a Reaction conditions: 0.5 g lignin, 0.5 g catalyst, 12.5 mL tetralin, microwaves, 400 W, average temperature 140 °C, 30 min reaction. The difference to 100 corresponds to gaseous products; not quantified in the systems.

Table 4Compounds identified in appreciable quantities in the obtained bio-oils. Compounds yields concentration in mg of each compound per gram of lignin.^a

| | Blank | Ni2%AlSBA | Ni5%AlSBA | Ni10%AlSBA | Pd2%AlSBA | Pt2%AlSBA | Ru2%AlSBA |
|---|-------|-----------|-----------|------------|-----------|-----------|-----------|
| Mesitol (2) | 0.56 | 2.26 | 1.19 | 1.13 | 0.49 | 1.67 | 1.40 |
| 2,3,6-Trimethylphenol (3) | 0.19 | 0.76 | 0.22 | 0.28 | 0.18 | 0.17 | 0.45 |
| 6-Ethyl- <i>o</i> -cresol (5) | 0.13 | 0.14 | 0.04 | — | — | 0.32 | 0.19 |
| 4-Ethyl- <i>m</i> -cresol (6) | — | 0.11 | 0.04 | — | — | 0.08 | — |
| Vanillin (7) | 0.20 | 0.20 | 0.19 | 0.20 | — | 0.13 | 0.11 |
| Diethylphthalate (10) | 2.34 | 10.10 | 1.67 | 1.69 | 10.93 | 10.66 | 7.44 |
| 3,4-Dimethoxyphenol (11) | 0.05 | 0.12 | 0.05 | 0.15 | 0.24 | 0.09 | 0.09 |
| Syringaldehyde (12) | 0.47 | 0.68 | 0.57 | 0.56 | 0.15 | 0.43 | 0.43 |
| Butyl-octyl ester phthalic acid (16) | 0.21 | 0.36 | 0.30 | 0.19 | 0.34 | 0.36 | 0.37 |

^a Reaction conditions: 0.5 g lignin, 0.5 g catalyst, 12.5 mL tetralin, microwaves, 400 W, average temperature 140 °C, 30 min reaction.

or quantification as they were obtained in relatively low quantities (generally < 10% yield).

The bio-oil was subsequently analysed by GC-MS to determine the nature and concentration of the isolated simple phenolic

monomers (Tables 4 and 5, and Fig. 1). Apart from tetralin as reaction solvent, diethyl phthalate (**10**) and butyl-octyl phthalate (**16**) ester were also found in the bio-oil. These products have been formed from tetralin due to the reaction conditions used

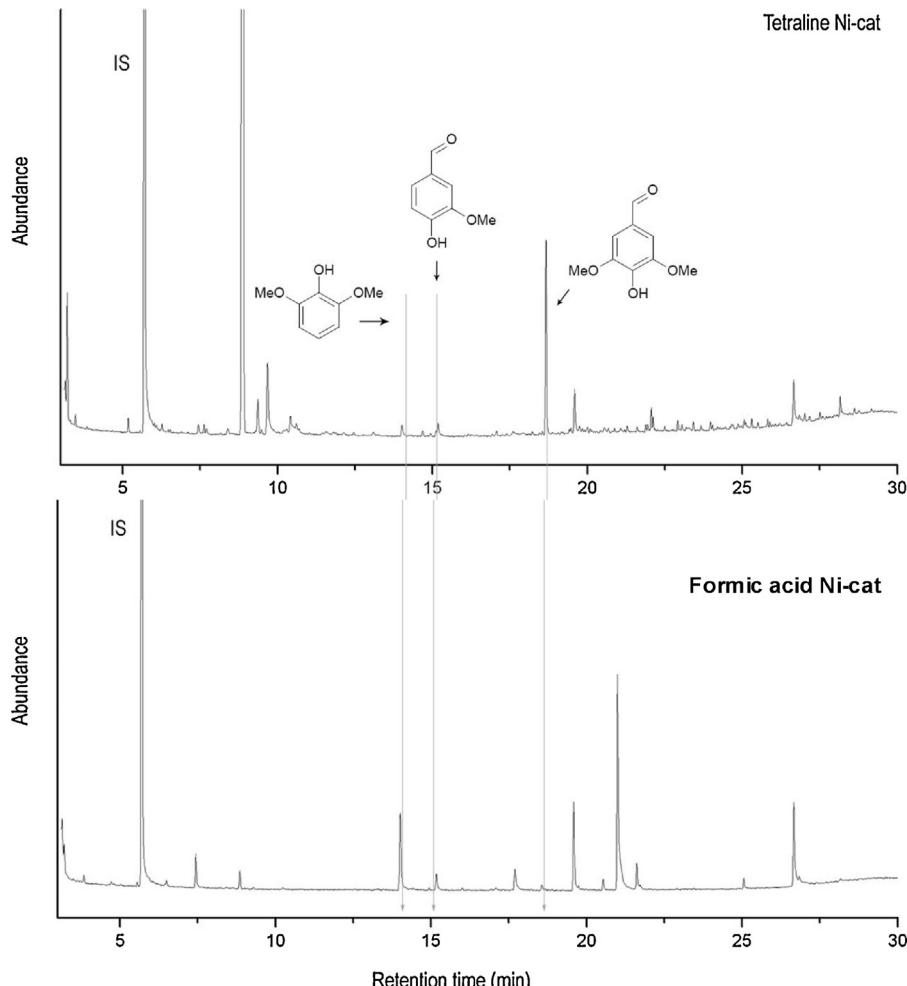


Fig. 4. GC-traces of Ni10%AlSBA catalysed organosolv lignin hydrogenolytic depolymerisation under microwave irradiation, showing some of the products observed by GC-MS analysis.

Table 5

Compounds present in the lignin-derived bio-oil for experiments carried out with the optimised Ni10%AlSBA catalyst using tetralin and formic acid, respectively. Compounds yields concentration as mg of each compound obtained per gram of lignin.

| Compound | Tetralin blank | Tetralin Ni cat. | Formic acid blank | Formic acid Ni cat. |
|--|----------------|------------------|-------------------|---------------------|
| Guaiacol (1) | – | – | 0.27 | 0.31 |
| Mesitol (2) | 0.56 | 1.13 | – | – |
| 2,3,6-Trimethoxyphenol (3) | 0.19 | 0.28 | – | – |
| Syringol (4) | 0.05 | 0.15 | 0.50 | 1.02 |
| Vanillin (7) | 0.20 | 0.20 | 0.24 | 0.22 |
| Acetovanillone (apocynin) (8) | – | – | 0.14 | 0.31 |
| 2,4'-Dihydroxy-3'-methoxyacetophenone (9) | – | – | 0.38 | 0.07 |
| Diethylphthalate (10) | 2.34 | 1.69 | – | – |
| Syringaldehyde (12) | 0.47 | 0.55 | 1.35 | 0.93 |
| Acetosyringone (13) | – | – | 0.08 | 0.11 |
| Desaspidinol (14) | – | – | 1.77 | 2.94 |
| Aspidinol (15) | – | – | 1.23 | 0.27 |
| Butyl-octyl phthalic acid ester (16) | 0.21 | 0.19 | – | – |
| G derivatives (1, 7, 8, 9, 10, 16) | 2.75 | 2.08 | 1.03 | 0.91 |
| S derivatives (2, 4, 12, 13, 14, 15) | 1.08 | 1.82 | 4.93 | 5.00 |

in this research (microwave assisted), with a important concentration diethyl phthalate produced at low metal concentrations (2 wt.%, **Table 4**). However, the origin of phthalates was not clear since diethyl phthalate has also been previously reported to be obtained under biodegradation of lignin under anaerobic and sulphate reducing conditions [22]. Deeper investigations about the origin of these products should be developed in order to clarify their origin.

Taking into account only the phenolic products of lignin origin, the main monomeric products were mesitol and syringaldehyde in tetralin experiments including blank runs. Vanillin (**7**) production could be associated to the release of guaiacyl intermediates. On the other hand, mesitol (**2**), 2,3,6-trimethylphenol (**3**) and syringaldehyde (**12**) had their origin in the release of syringyl units. Interestingly, the presence of some cresols could not be clearly understood. The absence of substituents in carbons adjacent to hydroxyl phenolic groups would suggest *p*-hydroxybenzyl origin but the presence of a substituent in *meta*- position with respect to hydroxyl phenolic groups could not be totally explained. Aspidinol [1-(2,6-dihydroxy-4-methoxy-3-methylphenyl)butan-1-one, compound **15**] detected in traces quantities in some tetralin experiments which comprise a C4 chain, is believed to be among the intermediates leading to the production of phthalates. Further investigations are currently ongoing under different conditions (in the presence and absence of dissolved oxygen) to find further evidences for these hypotheses.

The difference in quantities of products derived from guaiacyl units, syringyl units or *p*-hydroxyphenol units may be indicative of the proportions of each type of structure in the parent lignin (olive tree residues). It may also evidence differences in the way in which these types of units are hydrogenolysed under the selected conditions, which in fact seemed to be significantly influenced by the use of the hydrogen donating solvent (see bottom rows of **Table 5**). Tetraline exhibited a large amount of guaiacyl derivatives compared to syringyl as compared to a 5:1 syringyl to guaiacyl derivatives concentration ratio observed for formic acid (**Table 5**). Pepper and Leestated that the higher prevalence of products with guaiacyl origin could be correlated to syringyl units undergoing demethoxylation reactions to form guaiacyl derivatives [12]. These findings would suggest that demethoxylation reactions do not take place when formic acid is employed as hydrogen-donating solvent in lignin depolymerisation reactions.

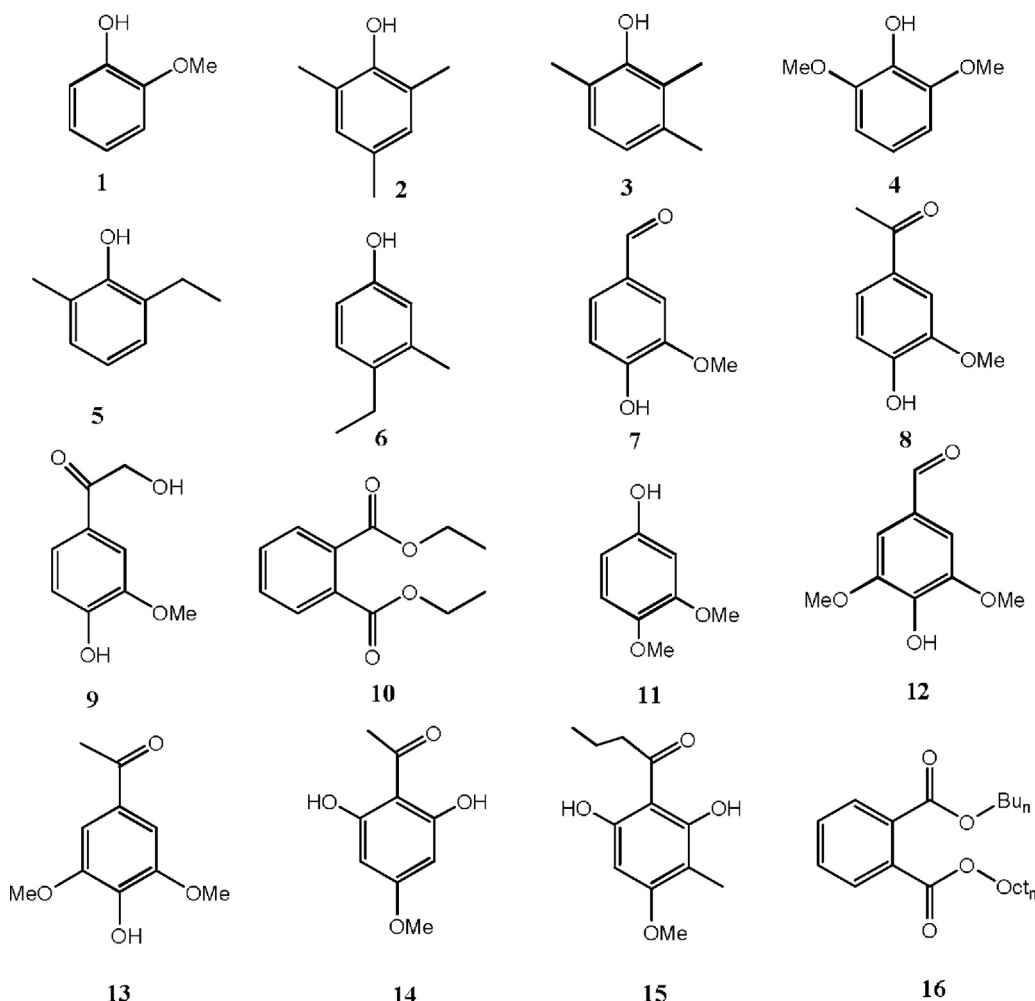
Cresol derivates were present in low yields for all the studied catalysts, even disappearing for Ni10%AlSBA and Pd2%AlSBA. Syringaldehyde yield also increased when using supported Nickel NPs as catalyst, while Pd NPs gave the worst results in the hydrogenolysis (still improving the yields of the blank run).

Compared to experiments using tetralin, the use of the optimum Ni10%AlSBA catalyst in conjunction with FA as hydrogen donating solvent promisingly changed the ratio and quantities of generated aromatics. Firstly, only traces of phthalates were found in FA experiments, with desaspidinol and aspidinol (**Scheme 1**, compounds **14, 15**) detected as major products in the hydrogenolytic process (**Table 5**). These findings confirmed the solvent (tetralin) origin of phthalates observed in tetralin experiments, from dehydration to naphtalene and then subsequent oxidation under the investigated conditions. Syringaldehyde (**12**) and syringol (**4**) were also observed in appreciable quantities.

The principal reaction in the hydrogenolysis of lignin is the cleavage of ether linkages connecting the α -, β - and γ -carbon atoms of a side chain and the 4-position of a phenolic ring in an adjacent unit (**Fig. 5**). Depending on reaction conditions, carbon–carbon linkages may also be ruptured during hydrogenolysis especially at α - β and β - γ sites [23]. Compounds **2, 6, 7, 11** and **12** as well as their derivatives are likely to arise from such carbon–carbon cleavage reactions (dealkylation and/or deacylation-related reactions) which take place preferentially on the acid sites of the aluminosilicate support upon formation of these small compounds [6,24]. Comparatively, the structure of compounds **3, 5, 10** and **16** suggested that these underwent further demethylation reactions (where carbon–carbon cleavage of 4 ring position and α -alkyl chain may occur) due to the presence of Lewis acid sites as evidenced by Strassberger et al. [25]. Hydrogenation reactions in the metal sites can be in principle responsible for the lost of methoxy groups (above all in positions 2 and 6 of the aromatic phenolic ring) and may explain the presence of methyl groups in the respective structures. Structures **2, 3, 5** and **6** did not possess methoxy groups but methyl groups. These transformations are likely to be due to radical reactions in the depolymerisation process.

In view of the obtained compounds and chemistries taking place in the process, the formation of simple aromatics can be proposed to be formed in a two step mechanism catalysed by highly accessible metal sites in the external surface of the catalyst (in which hydrogenolysis takes place leading to a pool of intermediates and/or final aromatic compounds) which then due to their small sizes diffuse through the pores and/or further interact with the accessible acidic sites of the catalyst to generate the products present in the bio-oil.

Most importantly, the profile of monomeric products was found to be different from other studies results [11,14,26], and only relatively similar to those recently reported by Li et al. [9]. The difference may be associated to the use of rapid and homogeneous heating achieved under microwave irradiation, which is able to accelerate and favour the rates of reaction and influence



Scheme 1. Compounds found in isolated bio-oils. (1) Guaiacol; (2) mesitol; (3) 2,3,6-trimethylphenol; (4) syringol; (5) 6-ethyl-o-cresol; (6) 4-ethyl-m-cresol; (7) vanillin; (8) acetovanillone (apocynin); (9) 2,4'-dihydroxy-3'-methoxyacetophenone; (10) diethyl phthalate; (11) 3,4-dimethoxyphenol; (12) syringaldehyde; (13) acetosyringone; (14) desaspindol; (15) aspindol; and (16) butyl-octyl phthalate ester.

selectivities to products in reactions catalysed by supported metal nanoparticles. In fact, the conventionally heated reaction run under identical conditions provided very low bio-oil yields (<10%) in the system for the optimum Ni10%AlSBA catalyst, in good agreement with previously reported results [26]. NPs sizes might also influence yields to simple aromatics as well as bio-oil yields by means of an improved interaction of the metal sites with bulky lignin for highly accessible and relatively large (30–40 nm) metal nanoparticles obtained under mechanochemical ball milling conditions on the external surface of the aluminosilicate supports [15,20].

MALDI-TOF oil analyses to determine the molecular weight of the compounds present in the bio-oil were carried out as GC-MS could only detect low molecular weight and relatively low boiling point compounds. Results are depicted in Fig. 6. Considering that a prototype lignin subunit (e.g. phenylpropane syringol) has a molecular weight of 197 g mol⁻¹ and a phenylpropane guaiacol unit is about 166 g mol⁻¹, results from Fig. 6 clearly demonstrate that most of the obtained products were primarily monomers and dimers. In addition, these analyses provided insights into the degree of lignin depolymerisation. Blank runs were remarkably different to those obtained using catalysts.

Weak signals were mostly observed for the blank run (reference) indicating a poor degree of lignin depolymerisation. As expected, all catalysts exhibited more intense signals at low molecular weights to those of the reference, which confirmed that the addition of

a metal supported catalyst enhanced lignin depolymerisation by hydrogenolysis under the investigated mild reaction conditions.

Significant differences between catalysts could also be clearly noticed. Except for Ni10%AlSBA, MALDI-TOF analyses revealed that the abundance of monomers was generally low. Dimers were more abundant in all cases and some trimers could also be detected. In the case of Ni5%AlSBA, Pd2%AlSBA and Ru2%AlSBA, the presence of trimers was more significant. Ni10%AlSBA exhibited the most desirable MALDI-TOF profile as signals that corresponded to monomeric compounds were more intense and abundant compared to those of other investigated catalysts. In the case of the use of FA as hydrogen-donating solvent, MALDI-TOF experiments (not included) were very similar to those of tetralin.

3.3. Bio-char

Bio-char yields from lignin valorisation have been summarised in Table 3. In general, the addition of catalysts in the systems did not significantly reduce the quantities of bio-char produced. Such yields were high for all studied catalysts, reaching a maximum bio-char production for Ni10%AlSBA (38%, Table 3), which is likely due to its high metal content (see discussion below). Supported ruthenium nanoparticles gave the minimum bio-char yield (4%). Bio-char formation from lignin under mild reaction conditions is a consequence of the cleavage of labile lignin bonds such as alkyl-aryl

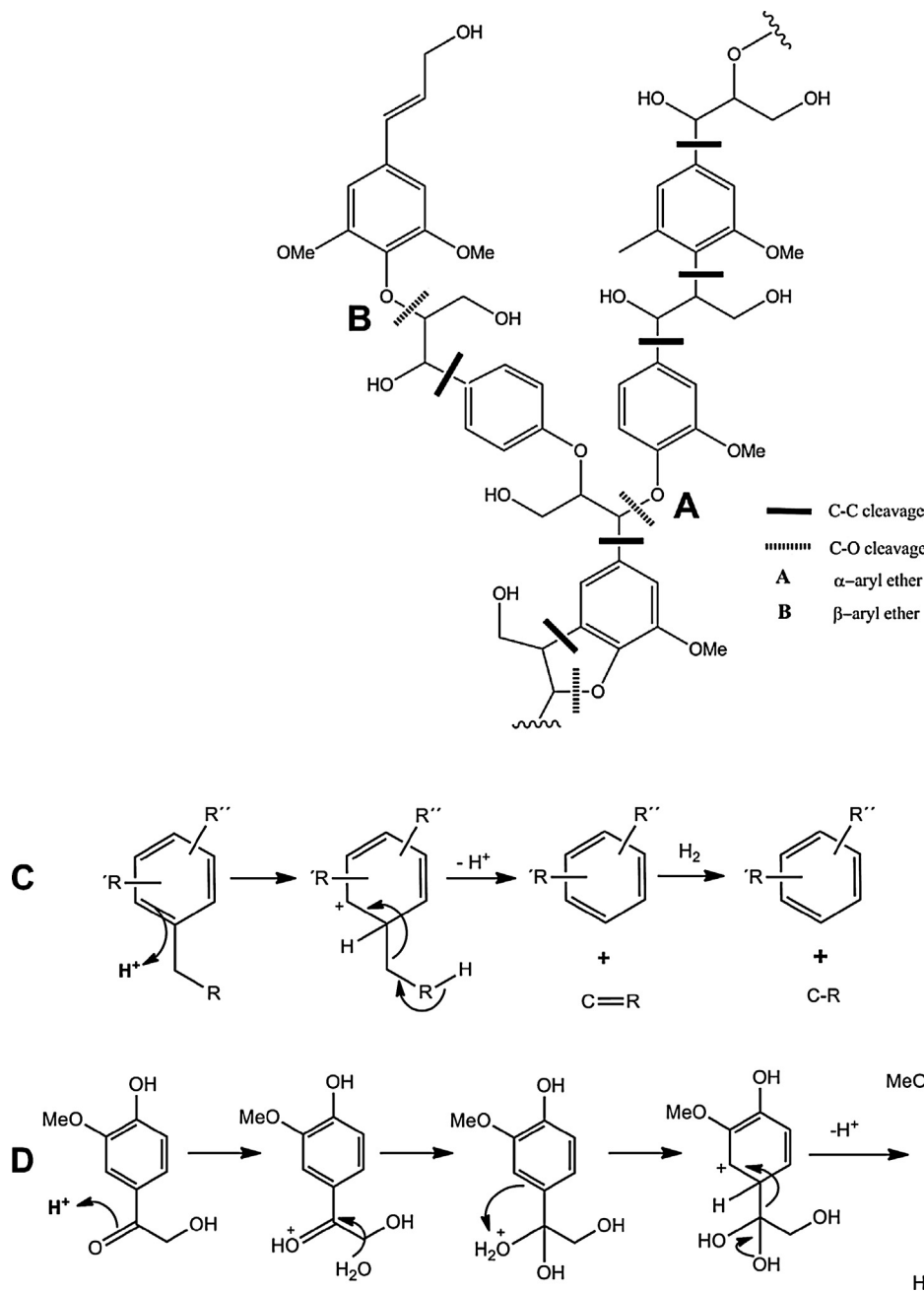


Fig. 5. Targeting C–C and C–O bond cleavage in lignin: the depolymerisation strategy (top scheme). Proposed acid-catalysed mechanisms for (C) hydrogenolysis of aromatic derivatives via dealylation and (D) deacylation of lignin-derived compounds.

Adapted from Ref. [6].

ether linkages and the resulting formation of more resistant condensed structures [27]. Microwave irradiation may have generated unstable fragments and/or radicals that could not be quenched in the hydrogen transfer reaction by tetralin, reacting between each other and forming complex structures, which generate high quantities of char for catalysts with high metal loadings (with the exception of Ni5%AlSBA). The bio-char obtained was not recovered for further analyses but in principle holds an interesting potential as by-product in the system and will be investigated in future studies. Comparatively, no bio-char was generated in experiments carried out with formic acid as hydrogen-donating solvent. These findings are most probably related to the efficient decomposition

of formic acid into CO, CO₂ and H₂ under microwave irradiation and the investigated conditions.

3.4. Residual lignin

Table 3 summarises the results of residual lignin yields in the microwave-assisted hydrogenolysis reactions. It is readily apparent that the content of residual lignin was high for all employed catalysts. However, the addition of supported metal nanoparticles as catalysts positively influenced the lignin hydrogenolytic depolymerisation. The residual lignin content for the ruthenium catalyst was the highest, taking into account only experiments where a

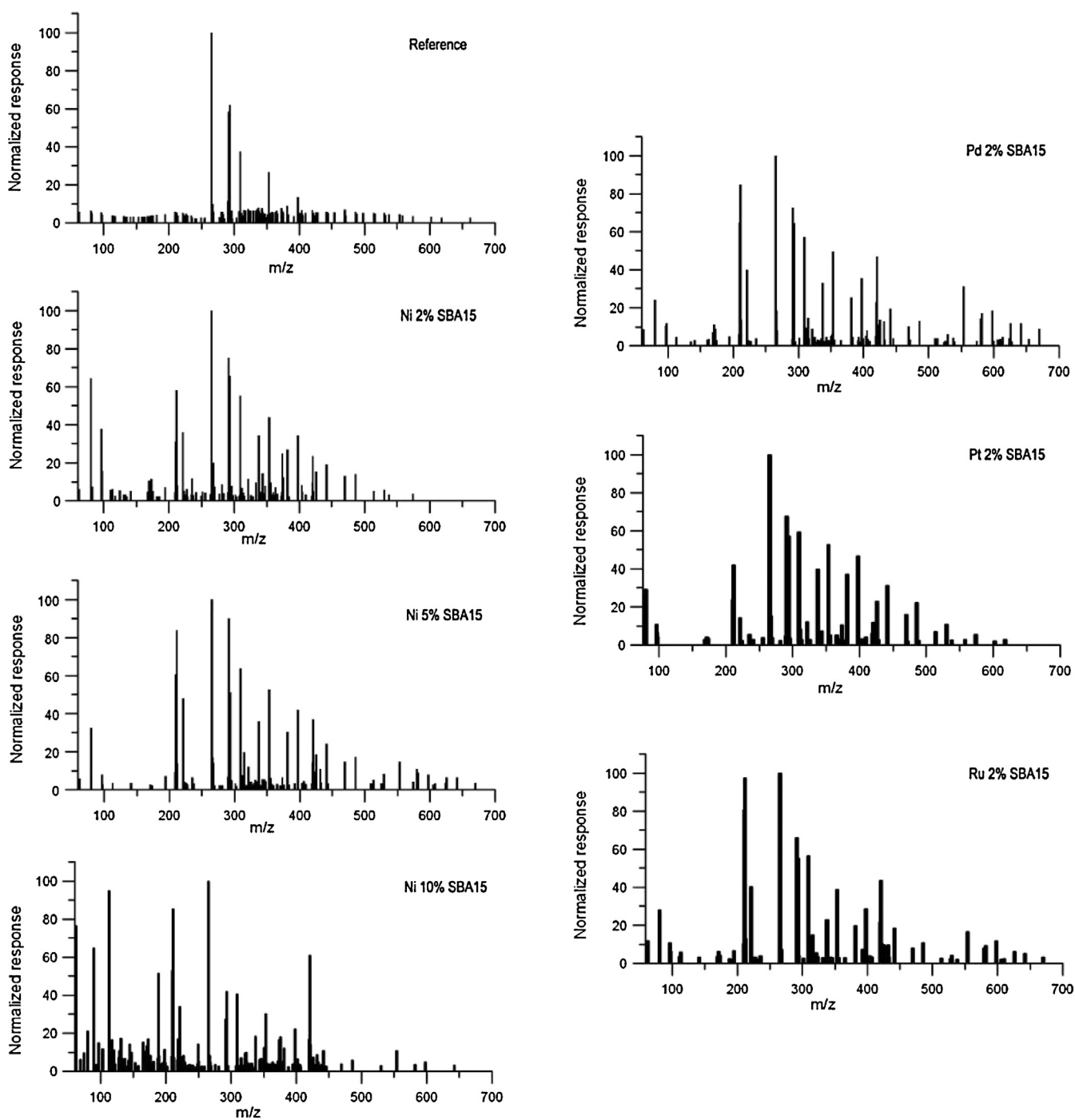


Fig. 6. MALDI-TOF oil analyses of all catalysts in the depolymerisation of lignin.

catalyst was added to the reaction. The best residual lignin content was obtained for Ni10%AlSBA, at the expense of its very high bio-char production. It is worth noting that the concept of residual lignin does not relate to conversion, which in turn means that a low residual lignin is not necessarily associated with a high concentration of phenolic monomers. Residual lignin decreased along with the increase of bio-char for most of the runs.

Residual lignins were subjected to high performance size exclusion chromatography in order to evaluate lignin behaviour during depolymerisation (Fig. 7 and Table 6). In all cases, two peaks were observed, a peak related to unconverted lignin and another peak (and a shoulder) corresponding to lower molecular weight lignins as a result of depolymerisation. The right plot (Fig. 7),

Table 6

HPSEC results of the recovered residual lignins in experiments using tetralin as well as formic acid (FA).

| Experiment | Mw | Mn | Mw/Mn |
|---------------------|--------|------|-------|
| Parent lignin | 7232 | 2125 | 3.40 |
| Blank (no catalyst) | 8549 | 2227 | 3.84 |
| Ni2%AlSBA | 5043 | 1828 | 2.76 |
| Ni5%AlSBA | 9663 | 1871 | 5.16 |
| Ni10%AlSBA | 3984 | 1231 | 3.24 |
| Ni10%AlSBA-FA | 5865 | 1618 | 3.62 |
| Pd2%AlSBA | 10,674 | 2002 | 5.33 |
| Pt2%AlSBA | 9806 | 1811 | 5.42 |
| Ru2%AlSBA | 14,396 | 2178 | 6.61 |

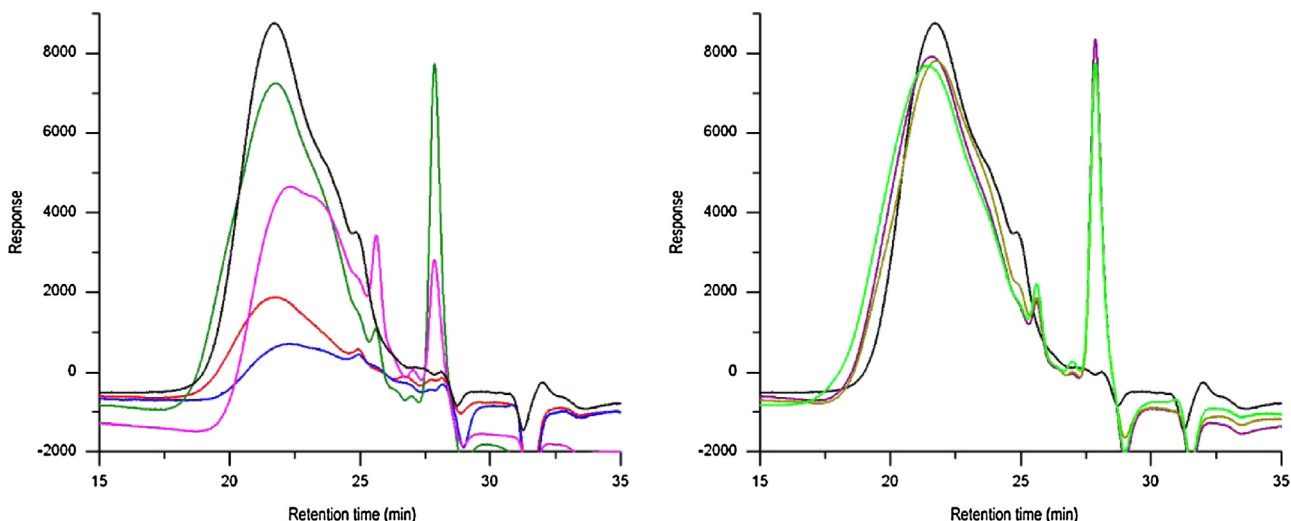


Fig. 7. Residual lignin HPSEC results for tetraline experiments. Left graphic: black (organosolv parent lignin), red (blank-no catalyst-), blue (Ni2%SBA15), olive green (Ni5%AlSBA) and magenta (Ni10%AlSBA). Right graphic: black (organosolv parent lignin), purple (Pd2%AlSBA), dark yellow (Pt2%AlSBA) and light green (Ru2%AlSBA). (For interpretation of the references to colour in this figure legend, the reader is referred to the web version of the article.)

representing palladium, platinum and ruthenium catalysts, showed that peaks corresponding to unconverted lignin appeared at shorter times to those of organosolv parent lignin, suggesting that repolymerisation had taken place. As in the bio-char case, microwave irradiation could have originated high radicals or unstable fragments (that could not be quenched under the reaction conditions) which reacted with the parent lignin structure. In fact, other authors have proposed the use of additional capping agents (e.g. boric acid) to minimise condensation of initially formed products under base-catalysed lignin processing [23a]. Blank experiments confirmed the repolymerisation trend of the parent lignin. Table 6 clearly summarises these findings and confirms that the nature of the supported metal strongly affected the occurrence of the depolymerisation phenomena.

Nickel catalysts comparably seemed to minimise repolymerisation phenomena as indicated by the presence of the unconverted lignin peak in residual lignins at the same retention time to that of the organosolv parent lignin. In particular, the peak corresponding to unconverted lignin from Ni10%AlSBA appeared at longer retention times, which points to a suppression of repolymerisation reactions together with a large degree of depolymerisation observed in this case. The nature and strength of the acid sites in the Al-SBA-15 support (required for dealkylation and/or deacylation-related reactions in the formation of the final products) were also carefully controlled to avoid secondary undesirable reactions of the generated aromatics (e.g. self-condensations, esterifications, acylations, etc.) which could lead to the formation of polycyclic aromatic species and thus partial repolymerisation species [6,23].

Average-weight molecular weights of nickel 2% and 10% experiments were those exclusively showing a decrease in molecular weight compared to parent organosolv lignin. This fact suggested a high depolymerisation degree for these two catalysts. In these experiments, polydispersity index (M_w/M_n) also decreased (referring to crude lignin), which is the normal trend in polymer degradation. These findings were in good agreement with MALDI-TOF analyses as well as with our hypotheses of the improved interaction metal-lignin observed for large clusters as Ni2% and Ni10%AlSBA materials exhibited in principle the largest NPs sizes (together with Pt).

Comparatively, Pd, Pt and Ru favoured repolymerisation phenomena yielding residual lignins with higher molecular weights to those of the parent organosolv lignin. Their

polydispersity index increased, rather than decreasing, proving the poor effect achieved on lignin depolymerisation using such noble metal catalysts.

Last and most importantly, our results also correlate well with those recently reported by Li et al. which pointed out the outperforming hydrogenolytic properties of Ni as compared to noble metal catalysts in lignocellulosics valorisation [9].

Elemental analyses of the residual lignins were also carried out in order to establish a carbon balance between parent organosolv and residual lignin. The objective was to evaluate changes in carbon content (Fig. 8). The carbon percentages in residual lignin of experiments with Ni5%AlSBA, Pd2%AlSBA, Pt2%AlSBA and Ru2%AlSBA increased as compared to the blank run without catalyst, indicating a poor depolymerisation of lignin. In addition, this growth will also confirm the repolymerisation phenomena observed during lignin hydrogenolysis in these experiments.

The elemental analysis of the residual lignin obtained in the reaction using Ni10%AlSBA revealed that this experiment reached the highest depolymerisation degree, indicated by a decreased in carbon content and the increase in oxygen content. These findings were also in good agreement with HPSEC and MALDI-TOF analyses which pointed out Ni10%AlSBA as optimum depolymerisation catalyst.

In terms of catalysts recycling, further studies are currently ongoing to fully optimise results but in principle catalysts are in principle stable and highly reusable under the investigated reaction conditions, with NP sizes remaining almost unaltered (no significant nanoparticle sintering) observed upon reused (Tables 1 and 7). Textural properties were also relatively well preserved as

Table 7

Nanoparticle sizes (as obtained in XRD patterns using the Scherrer equation) of fresh and spent catalysts in the microwave-assisted hydrogenolysis of lignin.

| Catalyst | NP sizes as obtained by XRD (nm) | |
|-----------------|----------------------------------|----------------|
| | Fresh | Spent catalyst |
| Ni2%/Al-SBA-15 | 42 | 42 |
| Ni5%/Al-SBA-15 | 25 | 29 |
| Ni10%/Al-SBA-15 | 40 | 45 |
| Pd2%/Al-SBA-15 | — | — |
| Pt2%/Al-SBA-15 | 37 | 38 |
| Ru2%/Al-SBA-15 | 17 | 23 |

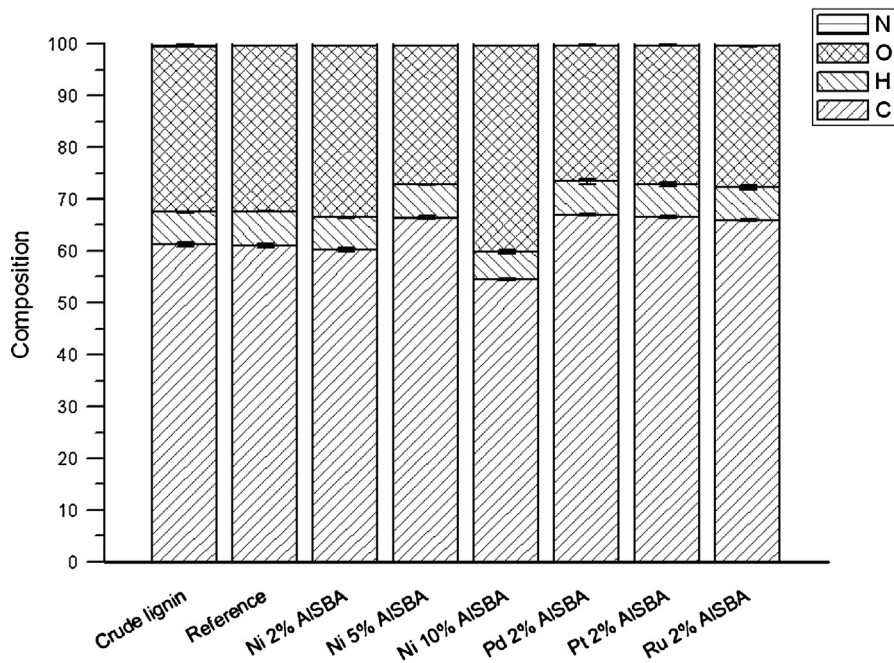


Fig. 8. Elemental analyses of residual lignins.

compared to the respective fresh catalyst (see example for Ni10%AlSBA), with only a certain decrease in surface area and pore volume. The conditioning step prior to catalyst reuse (thorough washing and conditioning with THF plus subsequent heating) ensures the efficient removal of residual lignin related species and aromatics physisorbed on/within the surface/pores of the catalyst due to their high solubility in THF (even the parent organosolv lignin is soluble in THF).

4. Conclusions

Organosolv lignin isolated from olive tree pruning was subjected to a heterogeneously catalysed mild hydrogenolytic depolymerisation approach assisted by microwave irradiation. A range of designer bifunctional catalysts featuring a combination of metal nanoparticles (Ni, Ru, Pd and Pt) supported on an acidic aluminosilicate (Al-SBA-15) were proved to provide access to simple phenolic products including mesitol and syringaldehyde. The nature and composition of the phenolic compounds was found to be influenced by the microwave irradiation, the type of metal employed in the catalysts as well as the hydrogen donating solvent employed in the process which changed the profile of expected obtained compounds. Ni10%AlSBA provided the optimum degree of lignin depolymerisation among all catalysts, which in general possessed high bio-char yields and residual lignin contents. Repolymerisation phenomena took place in most cases except for Ni-based catalysts, decreasing the production of phenolic monomer compounds. These results suggest that the proposed mild lignin hydrogenolysis approach could be improved.

In any case, the reported protocol is the first remarkably simple and environmentally sound report of lignin depolymerisation to date as it avoids the use of molecular hydrogen (thus minimising risks of explosions, leaks and related hazards), high-pressure devices and was carried out at mild reaction conditions (mild temperatures and short times of reaction) that can lead to over 30% bio-oil yield mostly enriched in monomeric and dimeric

phenolic compounds only after 30 min of reaction, which can have important consequences in the production of renewable gasolines and gasoline additives from lignin.

Acknowledgments

The authors would like to thank the Spanish Ministry of Science and Innovation (CTQ2010-19844-C02-02 and CTQ2010-18126) and Juan de la Cierva contract JCI-2011-09399 for supporting financially the project. Furthermore, the authors thank the technician Luis Bartolome of SGiker's for the elemental analyses. R.L. gratefully acknowledges support from Spanish MICINN via the concession of a RyC contract (ref. RYC-2009-04199) and funding under projects P10-FQM-6711 (Consejería de Ciencia e Innovación, Junta de Andalucía) and CTQ2011 28954-C02-02 (MICINN).

Appendix A. Supplementary data

Supplementary data associated with this article can be found, in the online version, at <http://dx.doi.org/10.1016/j.apcatb.2012.10.015>.

References

- [1] A. Sakakibara, in: T. Higuchi, H.M. Chang, T.K. Kirk (Eds.), *Recent Advances in Lignin Biodegradation Research*, UNI Publisher, Tokyo, 1983, p. 12.
- [2] J. Zakzeski, P.C.A. Bruijnincx, A.L. Jongerius, B.M. Weckhuysen, *Chemical Reviews* 110 (2010) 3552–3599.
- [3] M.P. Pandey, C.S. Kim, *Chemical Engineering & Technology* 34 (2011) 29–41.
- [4] (a) M.A. Aizenshtadt, K.G. Bogolitsyn, *Khimiya Rastitel'nogo Syr'ya* (2009) 5–18;
 (b) L. Zolia, M. Orlandi, D.S. Argyropoulos, *Journal of Agricultural and Food Chemistry* 56 (2008) 10115–10122;
 (c) A. Guerra, M. Norambuena, J. Freer, D.S. Argyropoulos, *Journal of Natural Products* 71 (2008) 836–841;
 (d) C. Crestini, D.S. Argyropoulos, *Bioorganic & Medicinal Chemistry* 6 (1998) 2161–2169.
- [5] (a) D.S. Argyropoulos, *Proceedings of the International Chemical Congress of Pacific Basin Societies (Pacificchem)*, December, Honolulu (Hawai), USA, 2010;
 (b) T. Nakamura, H. Kawamoto, S. Saka, *Journal of Wood Chemistry and Technology* 27 (2007) 121–133.
- [6] J.B. Binder, M.J. Gray, J.F. White, Z.C. Zhang, J.E. Holladay, *Biomass and Bioenergy* 33 (2009) 1122–1130.

- [7] A. Guerra, I. Filpponen, L.A. Lucia, C. Saquing, S. Baumberger, D.S. Argyropoulos, *Journal of Agricultural and Food Chemistry* 54 (2006) 5939–5947.
- [8] R.J.A. Gosselink, W. Teunissen, J.E.G. van Dam, E. De Jong, G. Gellerstedt, E.L. Scott, J.P.M. Sanders, *Bioresource Technology* 106 (2012) 173–177.
- [9] C. Li, M. Zheng, A. Wang, T. Zhang, *Energy & Environmental Science* (2012), <http://dx.doi.org/10.1039/c1ee02684>.
- [10] X. Wang, U. Richter, R. Rinaldi, *Proceedings of the 1st International Conference on Catalysis for Biorefineries*, Malaga, Spain, 2011.
- [11] D. Meier, R. Ante, O. Faix, *Bioresource Technology* 40 (1992) 171–177.
- [12] J.M. Pepper, Y.W. Lee, *Canadian Journal of Chemistry* 47 (1969) 723–727.
- [13] W.J. Connors, L.N. Johanson, K.V. Sarkanyen, P. Winslow, *Holzforschung* 34 (1980) 29–37.
- [14] R.W. Thring, J. Breau, *Fuel* 75 (1996) 795–800.
- [15] A. Pineda, A.M. Balu, J.M. Campelo, A.A. Romero, D. Carmona, F. Balas, J. Santamaría, R. Luque, *ChemSusChem* 4 (2011) 1561–1565.
- [16] A. Toledano, L. Serrano, J. Labidi, *Industrial & Engineering Chemistry Research* 50 (2011) 6573–6579.
- [17] (a) L. Liguori, T. Barth, *Journal of Analytical and Applied Pyrolysis* 92 (2011) 477–484;
 (b) N. Yan, C. Zhao, P.J. Dyson, C. Wang, L. Liu, Y. Kou, *ChemSusChem* 1 (2008) 626–629.
- [18] A. Sergeev, J.F. Hartwig, *Science* 332 (2011) 439–442.
- [19] J. Horacek, F. Homola, I. Kubickova, D. Kubicka, *Catalysis Today* 179 (2012) 191–198.
- [20] A. Pineda, A.M. Balu, J.M. Campelo, R. Luque, A.A. Romero, J.C. Serrano-Ruiz, *Catalysis Today* 187 (2012) 65–69.
- [21] (a) G.G. Couto, J.J. Klein, W.H. Schreiner, D.H. Mosca, A.J.A. de Oliveira, A.J.G. Zarbin, *Journal of Colloid and Interface Science* 311 (2007) 461–468;
 (b) Z. Fang, X. Qiu, J. Chen, X. Qiu, *Journal of Hazardous Materials* 185 (2011) 958–969.
- [22] J. Ko, Y. Shimizu, K. Ikeda, S. Kim, C. Park, S. Matsui, *Bioresource Technology* 100 (2009) 1622–1627.
- [23] A. Sakakibara, in: V.S.Y. Lin, C.W. Dence (Eds.), *Hydrogenolysis in Methods in Lignin Chemistry*, Springer-Verlag, Berlin, Heidelberg, 1992, pp. 350–368.
- [24] (a) V.M. Roberts, R.T. Knapp, X. Li, J.A. Lercher, *ChemCatChem* 2 (2010) 1407–1410;
 (b) V.M. Roberts, R.T. Knapp, X. Li, J.A. Lercher, *Applied Catalysis B* 95 (2010) 71–77;
 (c) V.M. Roberts, V. Stein, T. Reiner, A. Lemonidou, X. Li, J.A. Lercher, *Chemistry – A European Journal* 17 (2011) 5939–5948.
- [25] Z. Strassberger, S. Tanase, G. Rothenberg, *European Journal of Organic Chemistry* 27 (2011) 5246–5249.
- [26] K.M. Torr, D.J. van de Pas, E. Cazeils, I.D. Suckling, *Bioresource Technology* 102 (2011) 7608–7611.
- [27] A.M. Balu, D. Dallinger, D. Obermayer, J.M. Campelo, A.A. Romero, D. Carmona, F. Balas, J. Santamaría, K. Yohida, P.L. Gai, C. Vargas, C.O. Kappe, R. Luque, *Green Chemistry* 14 (2012) 393–402.